Variation Law of Water Film Thickness in Soil and Prediction Method for Unfrozen Water Content Postprint

Authors: Wan Xusheng

Date: 2022-01-26T18:07:48+00:00

Abstract

Changes in unfrozen water content directly influence the thermodynamic and deformation characteristics of frozen soil, and constitute a critical condition for hydro-thermal numerical computations. To investigate the variation law of unfrozen water content, the particle size distribution of soil is first characterized using equivalent particle size, and the soil is simplified into an equivalent particle size spherical packing system. Secondly, by considering the averaged packing arrangement of simple cubic packing and cubic closest packing, a calculation method for unfrozen water content in soil is proposed based on the premelting theory of porous media, and its rationality is verified through experimental data. Finally, the effects of impurity density and effective particle size on water film thickness and unfrozen water content are analyzed. The research results indicate that the free energy induced by surface charge density of soil particles, which alters water film thickness, is highly susceptible to impurity concentration; as the concentration increases, the influence of soil particle surface charge on the water film diminishes progressively. The liquid water content in soil is primarily determined by variations in water film thickness on soil particle surfaces; when equivalent particles decrease, the proportion of unfrozen water volume calculated from interstitial water gradually increases, playing a more significant role at lower concentrations. For soils with larger particles, the unfrozen water content model demonstrates favorable predictive performance. When the equivalent particle sizes of silty clay, loess, and sand are reduced by factors of 0.28, 0.3, and 0.36, respectively, the calculated results of unfrozen water volume content show good agreement with experimental values.

Full Text

Variation of Water Film Thickness in Soil and Prediction Method for Unfrozen Water Content

WAN Xusheng, YAN Mengyu, LU Jianguo, YAN Zhongrui
(School of Civil Engineering and Geomatics, Southwest Petroleum University, Chengdu, Sichuan, China)

Abstract

Variations in unfrozen water content directly influence the thermodynamic and deformation properties of frozen soils and constitute a critical condition for coupled water-heat numerical simulations. To investigate the variation 规律 of unfrozen water content, this study first employs an equivalent particle size to characterize the particle size distribution of soils, simplifying the soil matrix into a spherical packing system of equivalent particles. Second, considering an averaged packing arrangement between simple cubic packing and cubic close packing, a calculation method for unfrozen water content in soils is proposed based on premelting theory in porous media, and its validity is verified through experimental data. Finally, the effects of impurity density and effective particle size on water film thickness and unfrozen water content are analyzed. The results demonstrate that the free energy induced by surface charge density of soil particles is highly susceptible to impurity concentration, with the influence of surface charge on water film thickness diminishing as concentration increases. The liquid water fraction in soils is primarily determined by variations in water film thickness on particle surfaces; as the equivalent particle size decreases, the volumetric proportion of unfrozen water contributed by interstitial water gradually increases, playing a more significant role at lower impurity concentrations. The model exhibits good predictive performance for coarse-grained soils. Calculated volumetric unfrozen water contents show good agreement with experimental values when the equivalent particle sizes of silty clay, loess, and sand are reduced by ____ times, respectively.

Keywords: premelting; unfrozen water content; equivalent particle size; impurity concentration; surface charge density

Introduction

China has extensive permafrost coverage, with the combined area of perennial and seasonal frozen soils exceeding ____ of the national territory [1]. Infrastructure development in cold regions faces frost heave and thaw settlement phenomena induced by water-heat interactions, which severely constrain the construction of highways, railways, and other structures. Water serves as the material basis for soil freezing-thawing processes, and changes in unfrozen water content directly affect the thermodynamic and deformation characteristics of frozen soils. Moreover, the relationship between unfrozen water content and temperature constitutes a necessary condition for coupled water-heat numerical simulations.

Experimental studies have demonstrated that unfrozen water in frozen soils is primarily influenced by soil type, external conditions (including temperature and pressure), salinity, and freeze-thaw processes [2-4]. The difficulty of water freezing increases with decreasing particle size, increasing salt content, decreasing liquid saturation, and increasing specific surface area of activated soil particles [5]. With continuous advancement in testing technologies, methods such as nuclear magnetic resonance (NMR), time domain reflectometry (TDR), and frequency domain reflectometry (FDR) [6] have been widely applied to measure unfrozen water content. These techniques establish relationships between signal values and temperature to determine unfrozen water content at different temperatures.

Shoop [7] considered the adsorption effect of ice on water in soil pores and improved the general soil freezing curve proposed by Zhang. Based on capillary pressure theory, Dall' Amico [8] combined the Clapeyron equation with the Genuchten soil-water characteristic curve to establish a relationship between the soil freezing curve and soil water potential, with subsequent researchers validating this approach [9]. Sheshukov and Niber [10] expanded the unfrozen water content prediction formula by incorporating a simplified Clapeyron equation and introducing residual water content into the soil-water characteristic curve. Other scholars have developed soil water freezing models under ideal ice formation conditions based on pore size distribution functions and the sequential freezing of pore water from large to small pores [11]. Hitchcock [12] explained temperature relationships in mesoporous materials based on homogeneous nucleation theory, pore blocking, and single-pore theory. Anderson [13] first discovered through extensive laboratory experiments that unfrozen water content decreases exponentially with temperature and proposed an empirical formula, which has since been further improved and developed [14-16].

The premelting phenomenon of ice crystals in porous media provides a new approach for determining unfrozen water content. The Clapeyron equation establishes the relationship between ice pressure, water pressure, and temperature, and has been widely applied in coupled water-heat model calculations [17]. This equation clarifies that water freezing primarily depends on changes in ice-water pressure. Wettlaufer [18] developed a premelting theory-based model for the liquid water fraction in uniformly-sized spherical particle packing systems at subzero temperatures, simplifying unfrozen water content as a function of supercooling. Wettlaufer [19] revealed the intrinsic relationship between ice-liquid interfaces and ice crystal surfaces, demonstrating that premelting behavior is significantly affected by impurities in the medium. Hendrik and Wettlaufer [20] considered the effects of impurity concentration and solid particle surface charge density in porous media, establishing a premelting theory for ideal uniform particle systems. However, due to the wide range of particle sizes in soils, premelting theory has not been widely applied to soils. This paper proposes a calculation method for volumetric unfrozen water content in soils based on existing premelting theory for porous media, and analyzes the effects of impurity concentration and particle size on unfrozen water content.

1. Premelting Theory

In an ideal packing system of uniform spherical solid particles, pure water fills the voids between solid particles. The solid particles are assumed to be homogeneous, isotropic, and have smooth surfaces, with all pore water transforming into ice crystals at ultra-low temperatures. Before premelting (ice crystal melting) occurs, all voids are filled with ice crystals. As temperature increases, ice crystals begin to melt, and water exists in two forms: film water and interstitial water, as shown in Fig. 1. Interstitial water primarily exists in the voids surrounded by ice crystals and soil particles, and its existence temperature is determined by the ice-liquid curved interface. Film water mainly exists at the contact surfaces between soil particle surfaces and ice crystals, and its thickness is determined by the Gibbs-Thomson relationship [21].

Fig. 1. Existence form of liquid water in porous medium

For soils, the system contains impurities (salts), and many types of soil particles have surface charges. Therefore, the effects of impurities and particle charges should be considered in porous media systems.

Based on premelting theory in porous media, Wettlaufer [18] first established relationships for two common packing arrangements: simple cubic packing (SC) and face-centered cubic packing (FCC), with particle arrangements shown in Fig. 2. The relationship between the liquid water fraction and film thickness, particle radius, and ice-liquid contact surface radius in the packing system is given by formulas (1) and (2):

$$f_l(SC) = \frac{3(4-\pi)g_b + 3p}{3R} + \frac{9r^2}{R^2}$$

$$f_l(FCC) = \frac{3p + 2(3-\pi/2)g_b}{3R} + \frac{9r^2}{R^2}$$

where: f_l represents the volumetric fraction of liquid water; p is the percentage of particles in total volume (packing density); g_b is the water film thickness between ice crystals and solid particles; R is the particle radius; r is the radius of the ice-liquid contact surface, which affects freezing temperature and can be determined through the Gibbs-Thomson relationship [21].

If system impurities and surface charges are not considered, the film thickness d on solid particle surfaces can be calculated using formula (3) [24,26]:

$$L_{wi}\rho_l 6\pi\Delta T$$

where: ΔT represents the degree of supercooling, i.e., the reduction in initial freezing temperature (deviation from T_m); L_{wi} is the latent heat of ice-water phase change ($\mathrm{J \cdot mol^{-1}}$); T_m is the freezing point temperature of pure water (273.15 K); ρ_l is the molar density of pore solution ($\mathrm{mol \cdot m^{-3}}$). The Hamaker constant affects the value of d, as different material contact forms influence the Hamaker constant.

For soils, the system contains impurities (salts), and many soil particle types have surface charges. Therefore, the effects of impurities and particle charges should be considered in porous media systems.

Wettlaufer and Hendrik [20] derived the relationship between water film thickness and supercooling in uniform particle packing systems containing impurities and charges, as given by formula (4):

$$\rho_l d = \frac{n_{im} e^2}{\varepsilon \varepsilon_0 k T_m} - \frac{A_H}{6\pi d^3} + \frac{q_s^2}{2\varepsilon \varepsilon_0 k T_m}$$

where: n_{im} is the impurity concentration on soil particle surfaces; ε is the relative permittivity of liquid water; ε_0 is the vacuum permittivity; $T_m = 273.15$ K; e is the electron charge; N_A is Avogadro' s constant; k is the Boltzmann constant; q_s is the fixed surface charge density on particles; ρ_l is the molar density of pore solution; R is the gas constant. In calculations, ρ_l can be considered constant. The first term represents the effect of impurity concentration, the second term represents interfacial free energy under dispersion forces, and the third term represents interfacial free energy related to particle surface charge.

The above theories provide a relatively complete solution for water freezing in uniform particle porous media. However, effective methods remain lacking for water freezing in soils composed of different particle sizes.

2. Research Methods

Due to the wide distribution of soil particle sizes (e.g., silty clay typically ranges from several micrometers to several millimeters), the application of existing premelting theory to soils is limited. Assuming soil particles are spherical and ignoring surface roughness by treating surfaces as ideal smooth spheres, we can proceed as follows. Based on the soil particle size distribution curve, a sufficiently small particle size range is selected. Typically, experiments measure the mass (volume) proportion ω_i of soil particles within a certain size range R_i relative to the total particle mass (volume). The particle distribution and size classification are shown in Fig. 3. According to reference [29], the particle distribution curves for loess and sand are shown in Fig. 4.

Fig. 3. Soil particle distribution of silty clay

Fig. 4. Soil particle distribution of loess and sand

Within the i-th particle size range, particles are assumed to be uniformly distributed with radius R_i. If structural differences in soil are not considered, the soil can be idealized as a mixture of these two particle packing types, and the unfrozen water content for this particle size can be solved using the combined formulas (1) and (2). The total unfrozen water content can then be calculated using formula (5):

$$f_l(SC) = \sum_i \left[p_i(SC) \frac{3(4-\pi)g_b + 3p_i}{3R_i} + \frac{9r_i^2}{R_i^2} \right]$$

$$f_l(FCC) = \sum_i \left[p_i(FCC) \frac{3p_i + 2(3-\pi/2)g_b}{3R_i} + \frac{9r_i^2}{R_i^2} \right]$$

where: r_i represents the ice-liquid contact surface radius for soil particles with radius R_i.

However, calculating using formula (5) is cumbersome as it requires repeatedly solving for unfrozen water content under different particle sizes. To address this issue, this paper proposes an equivalent particle size method based on the volume proportion of different particle sizes, as calculated using formula (6):

$$R_e = \sum_i (\omega_i R_i)$$

where: R_e represents the equivalent particle size of soil particles.

Soil particle arrangements in soil lie between SC and FCC packing. To further simplify calculations, this paper adopts an average packing arrangement, i.e., taking the average of formulas (1) and (2). Combining formula (4), the liquid water content in soil can be calculated using formula (7):

$$f_l = 1.896 \frac{g_b}{R_e} + 0.275p + 7.388 \frac{r^2}{R_e^2}$$

The curved radius r of the ice-liquid contact surface can be determined through formula (8):

$$r = \frac{2\gamma_{sl} T_m}{L_{wi} \rho_s \Delta T}$$

where: ρ_s is the molar density of ice crystals; γ_{sl} is the ice-liquid surface free energy.

For the latent heat of ice-water phase change, its variation is ignored within a small temperature range, taking $L_{wi} \approx 6000$ J $\cdot$ mol^{-1}.

As temperature increases and approaches the freezing point infinitely, ice crystals are assumed to be at the pore center and can be approximated as an infinitesimal point, as shown in Fig. 5. At this point, ice crystals have maximum water film thickness. The geometric relationship of particle packing can be used to establish the initial pore volume concentration under different soil particle packing arrangements.

Fig. 5. Schematic diagram of maximum thickness of water film

Taking silty clay from the Qinghai-Tibet Plateau as the research object, the initial freezing temperature is -0.2°C [31], which is attributed to ion concentration in the soil [32]. Based on the solution freezing point calculation formula [33], the initial ion concentration is estimated to be approximately 0.07 $\text{mol} \cdot \text{L}^{-1}$. Assuming the salt type in soil is typical sodium chloride, $N = 2$. Using the particle size distribution curve of silty clay in Fig. 3, the equivalent particle radius is _____ m according to formula (6). The impurity concentration n_{im} can be estimated as _____ $\text{mol} \cdot \text{m}^{-2}$ using formula (9).

The relationship between soil particle water film thickness and freezing temperature depression can be established using formula (4), with calculation results shown in Fig. 6.

Fig. 6. Curve of relationship between degree of supercooling and thickness of water film in soils

3. Results and Analysis

3.1 Variation of Water Film Thickness and Unfrozen Water Content in Soil General soil particles have surface charges. Taking silty clay from the Qinghai-Tibet Plateau as an example, with initial freezing temperature of -0.2°C [31], attributed to ion concentration in the soil [32]. Based on the solution freezing point calculation formula [33], the initial ion concentration is estimated to be approximately 0.07 $\text{mol} \cdot \text{L}^{-1}$. Assuming the salt type in soil is typical sodium chloride, $N = 2$. Using the particle size distribution curve of silty clay in Fig. 3, the equivalent particle radius is calculated according to formula (6). Based on formula (9), the impurity concentration n_{im} is estimated.

The relationship between soil particle water film thickness and freezing temperature depression can be established using formula (4), with calculation results shown in Fig. 6. The diagonal line in the figure represents the variation curve of supercooling with water film thickness, with points on the line indicating supercooling values at different water film thicknesses. It can be observed that water film thickness in soil has a linear relationship with temperature. To achieve small changes in water film thickness, greater supercooling or lower temperatures are required. Points K1 and K2 indicate that to achieve water film thicknesses of 15 nm and 22 nm, supercooling must reach -20°C and -30°C, respectively. If the initial freezing temperature of soil is -0.2°C and soil temperature is -30°C, the water film thickness changes only slightly. Below -30°C, water film thickness in soil changes very little, and temperatures in typical frozen soil regions rarely reduce water film thickness to a few nanometers. Therefore, when calculating unfrozen water content in soil, temperatures are typically considered in the range of 0°C to -30°C.

Particle surface charge differences are relatively small [30], so a uniform value is adopted in calculations. Using formula (6), the equivalent particle radii for loess and sand are calculated as _____ m and _____ m, respectively. The equivalent particle radius for clay is approximately _____ m.

Without considering supercooling of soil water, surface impurity concentration is assumed to be the same as the previously mentioned silty clay. Similarly, the relationship between water film thickness between ice crystals and supercooling can be established based on formula (4). The curved ice-liquid interface radius can be solved through formula (8). Substituting the values of water film thickness and curved interface radius into formula (7) allows solving for unfrozen water content in soil under different supercooling conditions.

When the equivalent radius is reduced by _____ times, the calculated values show good agreement with experimental data. The calculation results are shown in Fig. 7. The experimental data in the figure are all from silty clay of the Qinghai-Tibet Plateau [15,28,31-33]. It can be found that the calculated values match well with experimental values, especially during the intense ice-water phase change stage (0°C to -2°C), indicating that the improved formula can solve unfrozen water content in silty clay at negative temperatures.

Fig. 7. Comparison between the calculated and experimental values of unfrozen water content in silty clay

For further validation of model applicability, experimental values from different soil types including loess, sand, and clay were selected for comparison. Unfrozen water experimental data for different soil types are all from references [18,28,34-35], with calculation results shown in Fig. 8. It can be seen that the calculated values can well reflect the variation 规律 of unfrozen water. At lower temperatures (i.e., below -5°C), predicted values are higher than experimental values. For sand, calculated values match well with experimental values, with volumetric unfrozen water content decreasing rapidly and stabilizing. For clay, although calculated values reflect the trend, the error is larger, especially in the initial freezing temperature stage, mainly because clay particles are flake-shaped, which differs significantly from the assumed spherical shape.

Fig. 8. Comparison between the calculated and experimental values of different soils

3.2 Factors Affecting Water Film Thickness The effects of different physical-chemical interface energies on water film thickness are shown in Fig. 9. Dispersion forces, related to the Hamaker constant, affect water film thickness independently of impurity concentration. As water film thickness decreases, supercooling increases linearly. When water film thickness decreases to the nanometer scale, dispersion forces gradually become active. Impurity concentration has a significant effect on water film thickness changes. As concentration increases, it becomes increasingly difficult to reduce water film thickness under the same supercooling, indicating increased difficulty of water freezing. The effect of soil particle surface charge density on water film thickness is highly susceptible to impurity concentration. As concentration increases, the influence of surface charge on water film decreases. Conversely, when impurity concentration decreases to 0.01 $\mathrm{mol \cdot m^{-2}}$, the effect of particle surface charge density on water film changes in soil pores exceeds the effect of impurity concentration itself. When impurity concentration exceeds 1 $\mathrm{mol \cdot m^{-2}}$, the effect of surface charge density on water film is minimal and can be neglected in calculations. Additionally, according to formula (4), as particle surface charge density decreases, its effect on water film also decreases.

Fig. 9. Effect of different impurity concentration and physical chemical interface energy

3.3 Variation Patterns of Film Water and Interstitial Water and Influencing Factors The contributions of particle surface water film, interstitial water between ice crystals, and interstitial water to calculated unfrozen water content for silty clay are shown in Fig. 10. It can be observed that water freezing in soil is mainly determined by changes in water film thickness on soil particle surfaces. The effect of water film between ice crystals is smaller compared to that on soil particle surfaces, with calculated values differing by an order of magnitude. The effect of interstitial water in soil on unfrozen water content is minimal, and its contribution can be neglected.

Fig. 10. Construction of water film and interstitial water to calculation of unfrozen water content

When impurity concentration in soil changes or soil particle size changes (e.g., clay has finer particles than silty clay), assuming different concentrations and particle size conditions, the calculated unfrozen water content results are shown in Fig. 11. It can be found that under high concentration conditions (Fig. 11a), as the equivalent particle size of soil decreases, unfrozen water content increases, indicating that water is more difficult to freeze in fine-grained soils. Under low concentration conditions (Fig. 11b), similar patterns are observed, but the role of interstitial water in calculated unfrozen water content becomes increasingly significant as particle size decreases, exceeding the values calculated based on water film thickness between ice crystals over a wide temperature range. Additionally, calculation results show that finer equivalent particle sizes lead to lower initial freezing temperatures. At low concentrations, the ice-liquid curved interface plays a dominant role in initial water freezing, and this radius decreases as equivalent particle size decreases.

Fig. 11. Effect of concentration and particle radius on unfrozen water content

4. Discussion

Classic exponential or power function relationships [13-16] have large errors during the intense phase change stage (near the initial freezing temperature) because exponential functions do not converge at the freezing point, and model parameters vary significantly with different initial water contents. Prediction models combining soil-water characteristic curves and freezing characteristic curves [8-10] depend heavily on initial and residual water contents, with many parameters lacking clear physical meaning. In contrast, the improved model in this paper has clear physical parameters, considers soil particle size, impurity concentration, and particle surface charge characteristics, and involves the physical-chemical micro-mechanism of water freezing.

Wettlaufer [18] calculated unfrozen water content distributions in uniform-sized polystyrene powder and graphitized carbon black powder using premelting theory, finding good agreement with experimental values when radii were reduced by _____ times. Actual soil particle arrangements are complex, and particle shapes are not all spherical, with particle surfaces exhibiting certain roughness. This paper employs equivalent particle size in calculations. When equivalent radii of silty clay, loess, and sand are reduced by , , and _____ times respectively, calculated values match well with experimental values. For fine-grained clay, the difference between calculated and experimental values is larger. Additionally, the model does not consider special structures in fine-grained soils, such as honeycomb or flocculent structures, which differ from naturally arranged particle distributions and affect model accuracy. Meanwhile, the radius reduction approach in calculations has not been elaborated in detail. Therefore, particle shape, surface roughness, actual particle arrangement, and soil structure type will be addressed in future research on micro-scale water freezing.

5. Conclusions

This paper studied the variation of volumetric unfrozen water content in soil with temperature based on premelting theory in porous media, proposed a calculation method, and analyzed the effects of impurity concentration and particle size on water film thickness and unfrozen water content. The main conclusions are:

1. The unfrozen water content model shows good predictive performance for coarse-grained soils. When equivalent particle sizes of silty clay, loess, and sand are reduced by _____ times, respectively, calculated unfrozen water contents are close to experimental values, and the model can well predict liquid water content in soils under different supercooling conditions. For clay, the prediction error is larger.
2. The effect of soil particle surface charge density on water film thickness is highly susceptible to impurity concentration, with the influence of surface charge on water film decreasing as concentration increases. As impurity concentration increases, water film thickness increases under the same

supercooling, making water freezing more difficult.

3. In calculating unfrozen water content in soil, the effect of dispersion forces can be neglected. Water freezing is mainly determined by changes in water film thickness on soil particle surfaces. As equivalent particle size decreases, the volumetric proportion of unfrozen water contributed by interstitial water gradually increases, playing a more significant role at lower concentrations.
4. When impurity concentration on soil particle surfaces is less than 1 $\text{mol} \cdot \text{m}^{-2}$, soil water freezing temperature is determined by the ice-liquid contact surface radius, which decreases as equivalent particle size decreases. Smaller radii result in lower freezing temperatures.

References

[1] 冻土物理学, 2010. [Xu Xiaozhu, Wang Jiacheng, Zhang Lixin, et al. Frozen Soil Physics[M]. Beijing: Science Press, 2010.]

[2] 土体的冻胀和盐胀机理科学出版社, 1995. [Xu Xiaozhu, Wang Jiacheng, Zhang Lixin, et al. Mechanisms of Frost Heave and Soil Expansion of Soils[M]. Beijing: Science Press, 1995.]

[3] Kurylyk B L, Watanabe K. The mathematical representation of freezing and thawing processes in variably saturated, non-deformable soils[J]. Advances in Water Resources, 2013, 60: 160-177.

[4] Zhou J Z, Wei C F, Lai Y M. et al. Application of the generalized Clapeyron equation to freezing point depression and unfrozen water content[J]. Water Resources Research, 2018, 54(11): 9412-9422.

[5] 季节性冻土区土体冻融过程及其对水热因子的响应干旱区研究, 2019, 36(6): 1568-1575. [Wu Yiheng, Zhao Pengwu, Zhou Mei, et al. Freezing-thawing process of seasonal frozen soil and its response to moisture and temperature[J]. Arid Zone Research, 2019, 36(6): 1568-1575.]

[6] Kleinberg R L, Griffin D D. NMR measurement of permafrost: Unfrozen water assay, pore scale distribution of ice, and hydraulic permeability of sediments[J]. Cold Regions Science and Technology, 2005, 42(1): 63-77.

[7] 中国科学院大学力相互作用过程及数值模拟研究, 2015. [Pei Wansheng. Study of the Hydro-thermal-mechanical Interaction Process of Frozen Soil and Its Numerical Simulation[D]. Beijing: University of Chinese Academy of Sciences, 2015.]

[8] Kruse A M, Darrow M M, Akagawa S. Improvements in measuring unfrozen water in frozen soils using the pulsed nuclear magnetic resonance method[J]. Journal of Cold Regions Engineering, 2018, 32(1): 04017016. https://doi.10.1061/(ASCE)CR.1943-5495.000

[9] 水分与温度的关系干旱区研究, 2020, 37(3): 627-635. [Wu Qinqin, Mo Shuhong, Cheng Shengdong, et al. Study on the correlation between soil moisture and

temperature of different land uses in the loess area during a freezing-thawing period[J]. Arid Zone Research, 2020, 37(3): 627-635.]

[10] Anderson D M, Tice A R. Predicting unfrozen water content in frozen soils from surface area measurements[J]. Highway Research Record, 1972, 393: 12-18.

[11] McKenzie J M, Voss C I, Siegel D I. Groundwater flow with energy transport and water-ice phase change: Numerical simulations, benchmarks, and application to freezing in peat bogs[J]. Advanced Water Resources, 2007, 30(4): 966-983.

[12] Kong L M, Wang Y S, Sun W J, et al. Influence of plasticity on unfrozen water content of frozen soils as determined by nuclear magnetic resonance[J]. Cold Regions Science and Technology, 2020, 172: 102993. https://doi.org/10.1016/j.coldregions.2020.102993.

[13] Daanen R P, Nieber J L. Model for coupled liquid water flow and heat transport with phase change in a snowpack[J]. Journal of Cold Regions Engineering, 2009, 23(2): 43-68.

[14] Painter S L, Karra S. Constitutive model for unfrozen water content in subfreezing unsaturated soils[J]. Vadose Zone Journal, 2014, 13(4): 334-338.

[15] Chai M T, Zhang J M, Zhang H, et al. A method for calculating unfrozen water content of silty clay with consideration of freezing point[J]. Applied Clay Science, 2018, 161: 474-481.

[16] Shoop S, Bigl S. Moisture migration during freeze and thaw of unsaturated soils: Modeling and large scale experiments[J]. Cold Regions Science and Technology, 1997, 25: 33-45.

[17] Zhang X, Sun S, Xue Y. Development and testing of a frozen soil parameterization for cold region studies[J]. Journal of Hydrometeorology, 2007, 8: 690-701.

[18] Dall' Amico M, Endrizzi S, Gruber S, et al. A robust and energy conserving model of freezing variably saturated soil[J]. The Cryosphere, 2011, 5: 469-484.

[19] Watanabe K, Kito T, Wake T, et al. Freezing experiments on unsaturated sand, loam and silt loam[J]. Annals of Glaciology, 2011, 52: 1-6.

[20] Sheshukov A Y, Niber J L. One-dimensional freezing of nonheaving unsaturated soils: Model formulation and similarity solution[J]. Water Resources Research, 2011, 47(11): 11519. https://doi.org/10.1029/2011WR010512.

[21] Wang C, Lai Y M, Zhang M Y. Estimating soil freezing characteristic curve based on pore size distribution[J]. Applied Thermal Engineering, 2017, 124: 1049-1061.

[22] Xiao Z A, Lai Y M, Zhang J. A thermodynamic model for calculating the unfrozen water content of frozen soil[J]. Cold Regions Science and Technology, 2020, 172: 103011. https://doi.org/10.1016/j.coldregions.2020.103011.

[23] Hitchcock I, Holt E M, Lowe J P, et al. Studies of freezing-melting hysteresis in cryoporometry scanning loop experiments using NMR diffusometry and relaxometry[J]. Chemical Engineering Science, 2011, 66(4): 582-592.

[24] Cash J W, Dash J G, Fu H Y. Theory of ice premelting in mono-sized powders[J]. Journal of Crystal Growth, 1992, 123: 101-108.

[25] Wettlaufer J S. Impurity effects in the premelting of ice[J]. Physical Review Letters, 1999, 82: 2516. https://doi.org/10.1103/PhysRevLett.82.2516.

[26] Hendrik H G, Wettlaufer J S. Theory of ice premelting in porous media[J]. Physical Review E, 2010, 81: 031604: 1-13.

[27] Dash J G, Rempel A W, Wettlaufer J S. The physics of premelted ice and its geophysical consequences[J]. Review of Modern Physics, 2006, 78: 695-741.

[28] Tang L Y, Wang K, Jin L, et al. A resistivity model for testing unfrozen water content of frozen soil[J]. Cold Regions Science and Technology, 2018, 153: 55-63.

[29] Qiu E X, Wan X S, Qu M F, et al. Estimating unfrozen water content in frozen soils based on soil particle distribution[J]. Journal of Cold Regions Engineering, 2020, 34(2): 04020002, doi:10.1061/(ASCE)CR.1943-5495.0000208.

[30] 论推演及应用基于双电层模型冻土中未冻水含量理, 2019, 40(4): 1449-1456. [Jin Xiao, Yang Wen, Meng Xianhong, et al. Deduction and application of unfrozen water content in soil based on electrical double layer theory[J]. Rock and Soil Mechanics, 2019, 40(4): 1449-1456.]

[31] Wen Z, Ma W, Feng W J, et al. Experimental study on unfrozen water content and soil matric potential of Qinghai-Tibet silty clay[J]. Environmental Earth Science, 2012, 66(5): 1467-1476.

[32] Wan X S, Lai Y M, Wang C. Experimental Study on the Freezing Temperatures of Saline Silty Soils[J]. Permafrost and Periglacial Processes, 2015, 26(2): 175-187.

[33] Lu J G, Pei W S, Zhang X Y, et al. Evaluation of calculation models for the unfrozen water content of freezing soils[J]. Journal of Hydrology, 2019, 575: 976-985.

[34] 岩土力学冻土未冻水含量的量热法试验研, 2010, 31(12): 3758-3764. [Leng Yifei, Zhang Xifa, Yang Fengxue, et al. Experimental research on unfrozen water content of frozen soils by calorimetry[J]. Rock and Soil Mechanics, 2010, 31(12): 3758-3764.]

[35] 实验研究冰川冻土兰州黄土在冻融过程中水热输运, 1996, 18(4): 319-324. [Li Shuxun, Cheng Guodong, Liu Jimin, et al. Experimental study on heat and moisture transfer in Lanzhou loess during freezing-thawing processes[J]. Journal of Glaciology and Geocryology, 1996, 18(4): 319-324.]

Figures

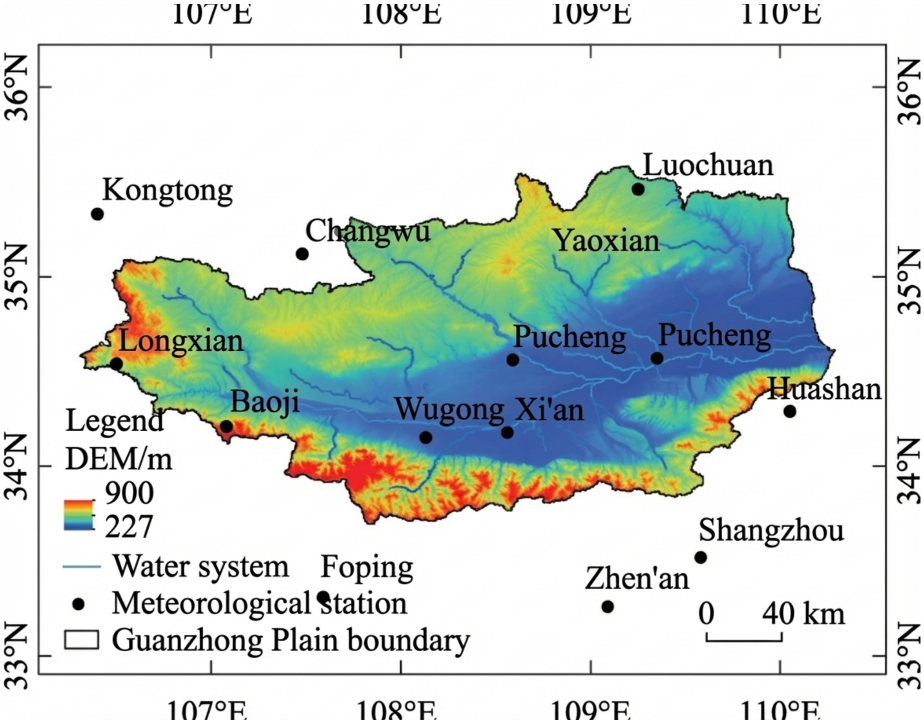

Figure 1: Figure 1

Source: ChinaXiv —Machine translation. Verify with original.

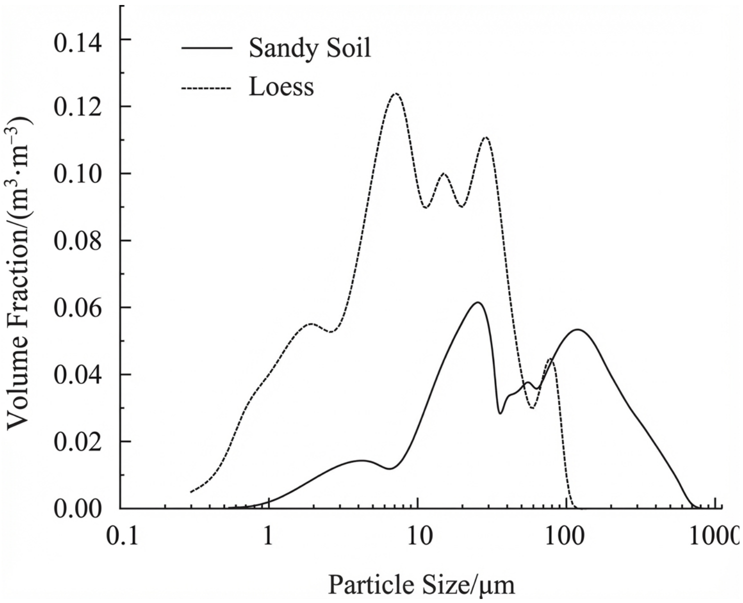

Figure 2: Figure 3

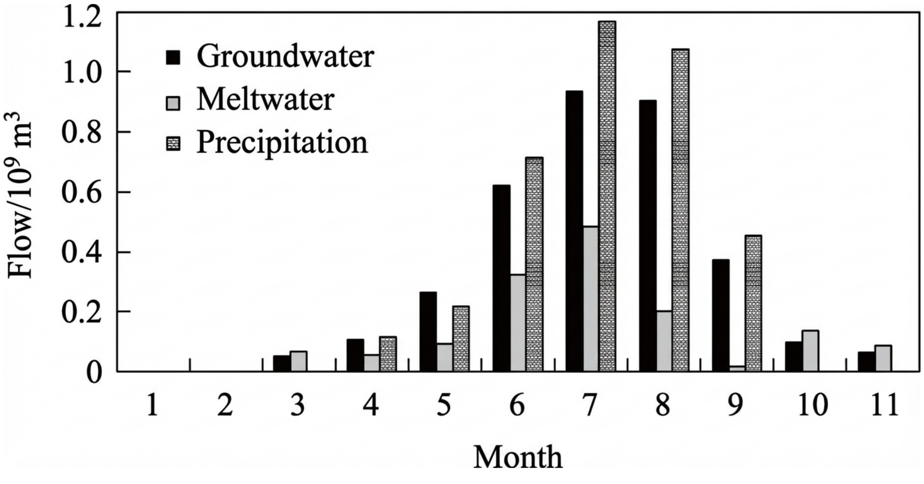

Figure 3: Figure 7

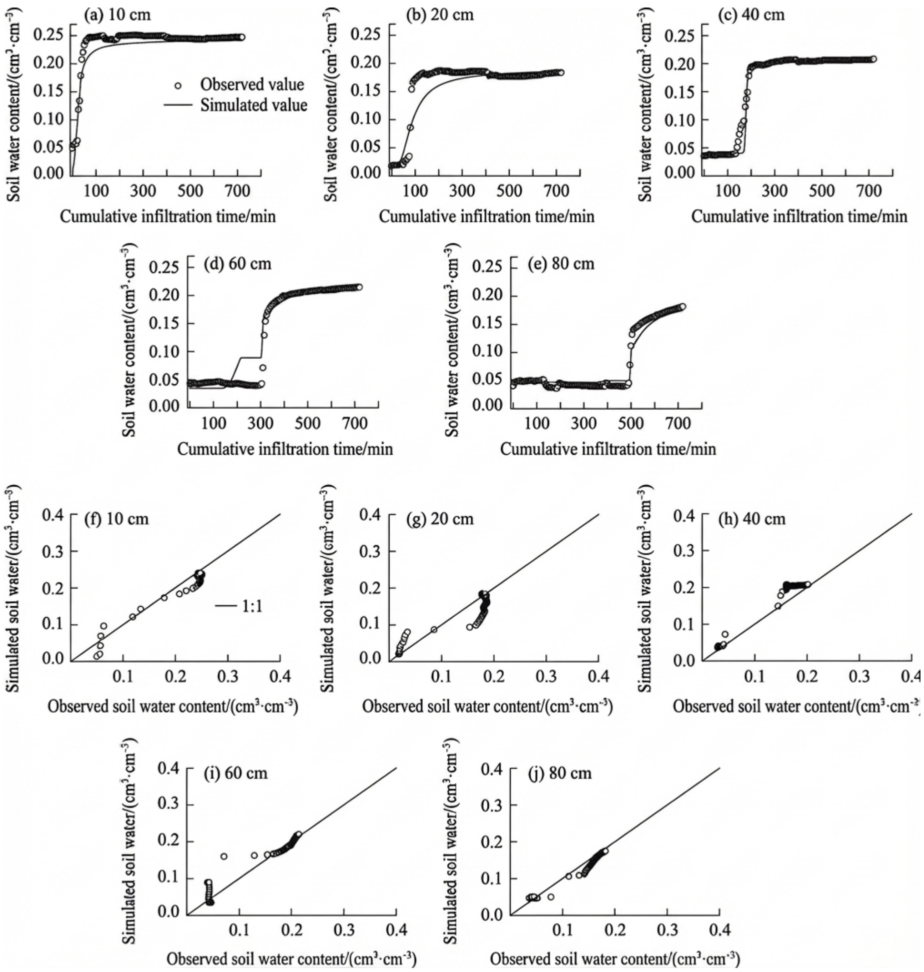

Figure 4: Figure 8

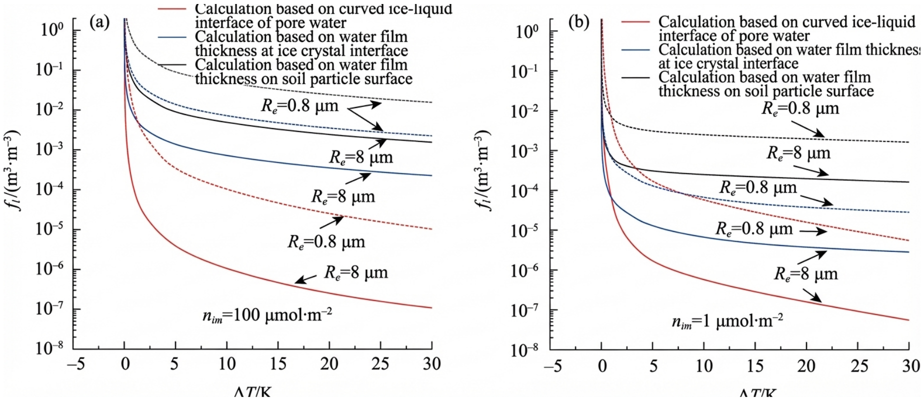

Figure 5: Figure 10

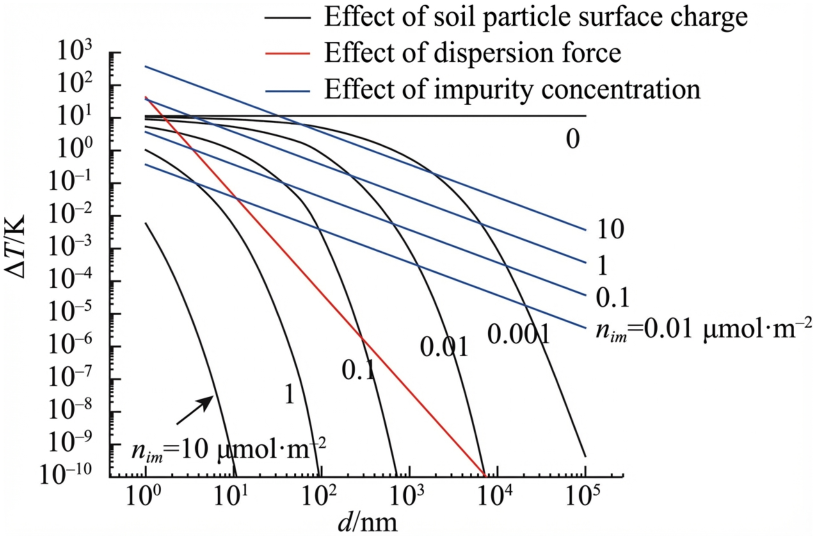

Figure 6: Figure 11